

FAU-TP 3-04/02
hep-th/0402014
May 22, 2019

Phase Diagram of the Gross-Neveu Model: Exact Results and Condensed Matter Precursors

Oliver Schnetz, Michael Thies¹ and Konrad Ulrichs
Institut für Theoretische Physik III
Universität Erlangen-Nürnberg, Erlangen, Germany

Abstract

Recently the revised phase diagram of the (large N) Gross-Neveu model in 1+1 dimensions with discrete chiral symmetry has been determined numerically. It features three phases, a massless and a massive Fermi gas and a kink-antikink crystal. Here we investigate the phase diagram by analytical means, mapping the Dirac-Hartree-Fock equation onto the non-relativistic Schrödinger equation with the (single gap) Lane potential. It is pointed out that mathematically identical phase diagrams appeared in the condensed matter literature some time ago in the context of the Peierls-Fröhlich model and ferromagnetic superconductors.

¹Electronic address: thies@theorie3.physik.uni-erlangen.de

1 Introduction

The Gross-Neveu (GN) model in 1+1 dimensions [1] is probably the simplest interacting fermionic field theory one can write down,

$$L = \bar{\psi}^{(i)} \partial_{\mu} \psi^{(i)} + \frac{1}{2} g^2 (\bar{\psi}^{(i)} \psi^{(i)})^2 \quad (1)$$

(here, $i = 1 \dots N$ is a flavor index, and the model is defined through the 't Hooft limit $N \rightarrow \infty$, $N g^2 = \text{const.}$ [2]). Yet, as evidenced by more than 900 citations in the hep-archive to date, this toy model has turned out to be quite valuable for a variety of physics questions (for a recent review and a discussion of subtleties associated with low dimensions, see Ref. [3]). If one solves it via semi-classical methods following the original 1974 paper, a surprising number of phenomena of interest to strong interaction physics unfold. Already in Ref. [1] asymptotic freedom, spontaneous breaking of the discrete chiral symmetry !, dynamical fermion mass generation and a scalar qq bound state (the π^0 meson) were demonstrated. The version with continuous chiral symmetry, the two-dimensional Nambu-Jona-Lasinio model [4] (NJL₂) possesses an additional massless π^0 meson. Shortly afterwards, massive kink [5] and kink-antikink [6] type baryons were derived analytically in the discrete chiral model, whereas the NJL₂ model features massless baryons [7, 8]. Previously it was shown that chiral symmetry gets restored at finite temperature in a second order phase transition [9, 10].

In contrast to these early works, it took a rather long and winding road to determine the full phase structure of the GN model at finite chemical potential and temperature. In 1985, the first phase diagram was proposed [11], followed by a number of works elaborating on it (see e.g. [12, 13]). Its prominent features were two phases (massive and massless quarks), separated by a line of first and second order transitions meeting at a tricritical point. In a density-temperature plot, a mixed phase would appear in the region of low density and temperature. It can be pictured as droplets of chirally restored vacuum containing extra quarks, embedded in the symmetry broken vacuum | reminiscent of the MIT bag model [14]. At the first order phase transition, the droplets fill all space [3].

This scenario as well as the underlying phase diagram were believed to hold for both variants of the GN model (with discrete and continuous chiral symmetry) [13]. Only in 2000 it was noticed that the phase diagram was hard to reconcile with the known baryon spectrum. In the case of the NJL₂ model, a thermodynamically more stable solution of the mean field equations turned out to be one where the chiral condensate assumes a helical form, namely a circle in the $(\mu; \phi)$ plane superimposed with a uniform translation along the ϕ axis (a "chiral spiral" [15]). Since the winding number is equal to baryon number, one can regard this structure as a caricature of a Skyrme crystal [16], a point of view emphasized in Ref. [15]. This helical order parameter was subsequently confirmed in Ref. [17], the (substantially) modified phase diagram of the NJL₂ model is discussed in Ref. [3].

As the bosonization technique based on the massless boson is unavailable in the GN model with discrete chiral symmetry, it took somewhat longer to construct a satisfactory phase diagram for this model. Following a variational calculation which clearly showed

the existence of a crystal ground state at $T = 0$ and any finite density [18], the full phase diagram was obtained in Ref. [19], based on a numerical solution of the Dirac-Hartree-Fock equations. The main new feature is the appearance of a third phase, a kink-antikink crystal, in addition to the two previously known homogeneous phases. It supersedes the mixed phase in the old phase diagram. All transitions are second order, and the tricritical point gets transmuted into a Lifshitz point characteristic for the transition from an inhomogeneous to a homogeneous ordered phase in condensed matter physics [20]. The mechanism which drives the spontaneous breakdown of translational invariance at finite density was identified as Overhauser effect [21] with gap formation at the Fermi surface. More recently, guided by these results, the analytic form of the self-consistent scalar potential at $T = 0$ has been guessed correctly and the self-consistency of the crystal ground state could be established analytically [22]. Many of the previous numerical results can now be written down in a concise, analytical way. Instrumental for this solution was the fact that by using an appropriate scalar potential expressed in terms of Jacobi elliptic functions, the Dirac-Hartree-Fock equation could be mapped onto a Schrödinger equation with the Lamé potential which was solved analytically long time ago [23].

In this paper, we extend the work of Ref. [22] to finite temperature. It turns out that the ansatz for the self-consistent potential used in [22] is general enough to encompass the self-consistent potential at any temperature and chemical potential. Apart from the obvious benefit of analytic insight into the phase structure of the GN model, our results have proven helpful in uncovering some striking relationship between the GN model and certain problems in condensed matter physics, notably in the context of superconductivity.

This paper is organized as follows: In Sect. 2, we present our two-parameter ansatz for the scalar potential and the solution of the Hartree-Fock-Dirac equation. In Sect. 3, we minimize the grand canonical potential. Sect. 4 contains the calculation of selected observables, in particular the scalar potential and the baryon density. In Sect. 5, we outline the formal proof of self-consistency at finite temperature and chemical potential. In Sect. 6, we map out the phase boundaries by appropriate series expansions and derive an effective action of Ginzburg-Landau type near the multicritical point. Finally in Sect. 7 we point out the close relationship between the phase diagram of the GN model and quasi-one-dimensional condensed matter problems.

2 Ansatz for the scalar potential and solution of the Dirac-Hartree-Fock equation

Our starting point is the Dirac-Hartree-Fock equation,

$${}^5 \frac{1}{i} \frac{\partial}{\partial x} + {}^0 S(x) \psi(x) = ! \psi(x); \quad (2)$$

with the following choice of matrices,

$${}^0 = \begin{pmatrix} 0 & 0 & 0 & 0 & 0 \end{pmatrix}; \quad {}^1 = \begin{pmatrix} 0 & 0 & 0 & 0 & 0 \end{pmatrix}; \quad {}^5 = \begin{pmatrix} 0 & 0 & 0 & 0 & 0 \end{pmatrix}; \quad (3)$$

In the Gross-Neveu model with discrete chiral symmetry, $S(x)$ is real. In terms of the upper and lower spinor components the Dirac equation consists of two coupled equations

$$\frac{\partial}{\partial x} S = ! \quad ! \quad (4)$$

which can be decoupled by squaring,

$$\frac{\partial^2}{\partial x^2} \frac{\partial S}{\partial x} + S^2 = !^2 : \quad ! \quad (5)$$

Eqs. (2-5) fall into the pattern of supersymmetric (SUSY) quantum mechanics. As our ansatz for $S(x)$, we choose the superpotential of the Lame potential [24],

$$S(x) = A^{-2} \frac{\text{sn}(Ax; \beta) \text{cn}(Ax; \beta)}{\text{dn}(Ax; \beta)} \quad A S(Ax) : \quad (6)$$

Here, various Jacobi elliptic functions with modulus appear [25]. Denoting the rescaled spatial variable Ax by ζ , $S(\zeta)$ has period $2K$ and moreover satisfies

$$S(\zeta + K) = -S(\zeta) \quad (7)$$

(K is the complete elliptic integral of the first kind). Owing to the ansatz (6), the second order equation (5) becomes

$$\frac{\partial^2}{\partial \zeta^2} + 2^{-2} \text{sn}^2(\zeta; \beta) = E_+ \quad ! \quad (8)$$

with

$$E = \frac{!^2}{A^2} + \beta^2 ; \quad (9)$$

the simplest case of the Lame equation (single gap). The solutions in terms of Jacobi functions are well known [23, 26],

$$_+ = N \frac{\#_1(v + w; q)}{\#_4(v; q)} e^{-z(\zeta)} ; \quad (10)$$

with

$$v = \frac{w}{2K} ; \quad w = \frac{z}{2K} ; \quad q = \text{ nome}(\beta) : \quad (11)$$

The parameter is related to the energy eigenvalue as follows,

$$\text{dn}^2(\zeta; \beta) = E_+^{-2} : \quad (12)$$

For the upper band, $\beta = i$; for the lower band, $\beta = K + i$, where β runs from 0 to $K^0 = K(1 - \beta^2)$. Once β is given, z follows from the Dirac equation (4),

$$= \frac{A}{!} \frac{\partial}{\partial \zeta} + S(\zeta) \quad _+ : \quad ! \quad (13)$$

Using various identities, one can deduce that

$$() = e^{K Z ()} + (+ K) \quad (14)$$

where the sign refers to positive/negative energy states. This relation is intimately connected to the symmetry property (7) which implies that the Dirac Hamiltonian is invariant under a combined translation by K and a discrete chiral transformation. Eq. (14) then merely expresses the fact that the wave functions belong to an irreducible representation of this symmetry group (\mathbb{Z}_2 is purely imaginary). Applying the transformation twice yields

$$+ (+ 2K) = e^{2K Z()} + (); \quad (15)$$

in agreement with the Bloch form of the solution (10) given in [26]. We still have to determine the normalization factor N in Eq. (10). In a continuum normalization, the spatially averaged fermion density should be normalized to 1 for each level,

$$1 = h^y \quad i = \frac{1}{2K} \sum_{j=0}^{2K} d_{2j+1} : \quad (16)$$

Inserting expression (10) and using an addition theorem for $\#_1$ [27],

$$\#_3^2(0)\#_1(x+y)\#_1(x-y) = \#_4^2(x)\#_2^2(y) \quad \#_2^2(x)\#_4^2(y) \quad (17)$$

together with standard relations between different Jacobi functions, one finds

$$j + \frac{\partial}{\partial A} = \frac{1 - \frac{\partial^2}{\partial A^2}}{1 - \frac{\partial^2}{\partial A^2}} \quad (18)$$

with

$$A = \frac{\#_2^2(w; q)}{\#_3^2(0; q)} : \quad (19)$$

Now the direct integration can be carried out with the result,

$$1 = \frac{2\mathfrak{N} \mathfrak{J}^2 A}{2 \mathfrak{C} n^2(\mathfrak{z})} \quad dn^2(\mathfrak{z}) \quad \frac{E}{K} \quad ! \quad (20)$$

(E is the complete elliptic integral of the second kind). This determines the normalization factor \sqrt{f} .

Let us now compute scalar and baryon densities for a single orbit. In our representation where $\psi^0 = \psi_1$, the scalar density is given by

$$= \quad (\quad + \quad + \quad) = \quad \frac{1}{A} \frac{P}{E} \frac{\overline{E^2}}{E-K} S(x) \quad (21)$$

for positive/negative energy states, respectively. We have inserted the expressions for α and β and eliminated $d\alpha(\cdot)$ in favor of the energy E , cf. Eq. (12). Notice that every orbit yields the same x -dependence. This will be of great help in proving the self-consistency of $S(x)$ below.

On the other hand, using Eqs. (18), (20) and (14), the baryon density can be represented as

$$y = \frac{E^2 \frac{dn^2(\cdot)}{E^2} + dn^2(\cdot + K)}{E^2} : \quad (22)$$

Upon calculating the spatial average

$$\bar{dn}^2(\cdot) \approx E = K \cdot \quad (23)$$

we can see that it is correctly normalized, see Eq. (16).

3 Minimization of the grand canonical potential

For independent fermions as appropriate for the relativistic Hartree-Fock approximation, the grand canonical potential density (per flavor) is given by (see [3] and references therein)

$$= - \frac{1}{0} \int_0^Z \frac{dp}{h} \ln \frac{1 + e^{-(\cdot)}}{1 + e^{(\cdot)}} + \frac{1}{2N g^2} \int_0^Z dx S^2(x); \quad (24)$$

Here,

$$= j! \cdot j = A^p \frac{p}{E^2}; \quad (25)$$

≈ 2 is an ultra-violet cutoff, $\approx 2K$ is the spatial period of $S(x)$, and we work in units where the dynamical fermion mass in the vacuum is 1. In order to perform the renormalization, we isolate the divergent part as usual,

$$\ln(1 + e^{(\cdot)}) = (\cdot) + \ln(1 + e^{(\cdot)}); \quad (26)$$

This enables us to split up \approx into the ground state energy computed previously (corresponding to the $T = 0$ state of antimatter characterized by a Fermi momentum p_f , see Ref. [22]) and two integrals accounting for finite temperature effects,

$$= E_{gs} + I_1 + I_2 \quad (27)$$

with

$$\begin{aligned} E_{gs} &= - \frac{1}{0} \int_0^Z \frac{dp}{h} + \frac{1}{2N g^2} \int_0^Z dx S^2(x) \\ I_1 &= - \frac{1}{0} \int_0^{p_f} \frac{dp}{h} \\ I_2 &= - \frac{1}{0} \int_0^Z \frac{dp}{h} \ln \frac{1 + e^{-(\cdot)}}{1 + e^{(\cdot)}} \stackrel{!}{=} : \end{aligned} \quad (28)$$

We have dropped an irrelevant divergent term, ≈ 2 , originating from the density of the Dirac sea. We now assume that the scalar potential at finite T and \approx is given by the Lane superpotential (6). We can then take over the renormalized ground state energy from Ref. [22] (without invoking any relation between A and \approx though),

$$E_{gs} = \frac{A^2}{2} \cdot 1 - \frac{1}{2} \cdot 2 - 2 \frac{E}{K} \stackrel{!}{=} + \frac{A^2}{2} \cdot 1 - \frac{1}{2} \cdot 2 - \frac{E}{K} \stackrel{!}{=} \ln(A) : \quad (29)$$

Next, we evaluate I_1 in Eq. (28), integrating over the first band of the Lame spectrum and employing the known density of states [26],

$$I_1 = \frac{A^2}{2} \int_0^{\infty} \frac{p}{1 - \frac{E^2}{K^2}} \frac{1}{2} \frac{1}{2} \frac{E}{K} \ln \frac{1}{2} \frac{E^2}{2} \frac{p}{1 - \frac{E^2}{K^2}} \frac{!}{\#} \frac{dE}{E} : \quad (30)$$

The remaining integral I_2 depending on $(T; \mu)$ in Eq. (28) cannot be performed analytically. Inserting the density of states and the relation between μ and E , it can be written in compact form as follows,

$$I_2 = \frac{A}{2} \int_0^{\infty} \frac{Z_1}{E^2} \frac{Z_1}{1 + \frac{E^2}{K^2}} \frac{dE}{E} \frac{!}{\#} \frac{(E = K + \sqrt{E^2 - K^2})}{(1 - E)(E - \sqrt{E^2 - K^2})(1 + \sqrt{E^2 - K^2})} \frac{h}{1 + e^{(A^2 \frac{p}{E^2} - \mu) / kT}} \frac{i}{1 + e^{(A^2 \frac{p}{E^2} + \mu) / kT}} : \quad (31)$$

The integration limits reflect the two bands of the Lame spectrum.

For given $(\mu; T)$, one has to minimize the thermodynamic potential (27) with respect to A and μ . Superficially, this looks more involved than the corresponding calculation in the case of unbroken translational invariance where one has to minimize only with respect to one parameter, the physical fermion mass m . As a matter of fact, it turns out that there is no significant complication. To see how this comes about, let us first rescale the effective potential, the parameter A and the chemical potential as

$$\tilde{a} = \frac{A}{\sqrt{K^2 - E^2}} ; \quad a = \frac{A}{\sqrt{K^2}} ; \quad \tilde{\mu} = \frac{\mu}{\sqrt{K^2 - E^2}} : \quad (32)$$

A useful notation for the following manipulations is

$$\begin{aligned} {}^2E_{\text{gs}} &= a^2 G_2(\mu) + a^2 \ln(a = \tilde{a}) G_3(\mu) ; \\ {}^2I_1 &= a^2 G_1(\mu) ; \\ {}^2I_2 &= a F(a; \mu; \tilde{\mu}) ; \end{aligned} \quad (33)$$

with

$$\begin{aligned} G_1(\mu) &= \frac{1}{2} \frac{p}{1 - \frac{E^2}{K^2}} + \frac{1}{2} G_3(\mu) \ln \frac{1}{2} \frac{E^2}{2} \frac{p}{1 - \frac{E^2}{K^2}} \frac{!}{\#} \\ G_2(\mu) &= \frac{1}{2} \frac{1}{1 - \frac{E^2}{K^2}} \frac{1}{2} \frac{E}{K} G_3(\mu) (1 - \ln \frac{1}{2}) \\ G_3(\mu) &= \frac{1}{2} \frac{1}{1 - \frac{E^2}{K^2}} \frac{1}{2} \frac{E}{K} \\ F(a; \mu; \tilde{\mu}) &= \frac{1}{2} \frac{Z_1}{E^2} \frac{Z_1}{1 + \frac{E^2}{K^2}} \frac{dE}{E} \frac{!}{\#} \frac{(E = K + \sqrt{E^2 - K^2})}{(1 - E)(E - \sqrt{E^2 - K^2})(1 + \sqrt{E^2 - K^2})} \frac{h}{1 + e^{(a^2 \frac{p}{E^2} - \tilde{\mu}) / kT}} \frac{i}{1 + e^{(a^2 \frac{p}{E^2} + \tilde{\mu}) / kT}} \end{aligned} \quad (34)$$

Setting

$$G = G_1 + G_2 ; \quad (35)$$

we can express the grand canonical potential in the symbolic form

$$\sim = a^2 G + a^2 G_3 \ln \frac{a}{-} + a F : \quad (36)$$

We minimize \sim with respect to a and $(a$ prime stands for ∂ , a dot for ∂_a),

$$\begin{aligned} \partial_a \sim = 0 &= 2aG + 2aG_3 \ln \frac{a}{-} + aG_3 + F + aF' ; \\ \partial \sim = 0 &= a^2 G' + a^2 G_3' \ln \frac{a}{-} + aF' ; \end{aligned} \quad (37)$$

Focussing on the non-trivial solution ($a \neq 0$) and eliminating $\ln(a =)$ from these two equations, we get the central equation in this approach,

$$G_3' 2aG + aG_3 + F + aF' - 2G_3 (aG' + F') = 0 : \quad (38)$$

$\ln(= a)$ can then be written in two equivalent ways,

$$\ln \frac{a}{-} = \frac{1}{2} + \frac{2aG + F + aF'}{2aG_3} = \frac{aG' + F'}{aG_3'} \quad (39)$$

The procedure is now the following:

1. Choose values for $(0:::1)$ and $(0:::1)$.
2. Solve Eq. (38) for a . This requires finding the zero's of a function of one variable given as a one-dimensional numerical integral.
3. Evaluate using Eq. (39).
4. The parameters $fA = a = ; ; = = ;$ then determine the scalar potential and all observables in one point in the $(T;)$ -plane.

This enables us to compute the phase diagram systematically and to explore limits of interest. Note that the translationally invariant solution is contained as a special case in this formalism; it corresponds to the limit $! 1$.

We have performed calculations along the lines sketched above. We illustrate the result of the minimization procedure by plotting lines of constant A and $$ in the $(; T)$ -plane, see Fig. 1. To clarify this diagram, we also show separately the lines $A = \text{const.}$ and $= \text{const.}$ in Figs. 2 and 3. The thick lines in Fig. 2 correspond to $A = 0$ (phase boundary between massive and massless phases) and $A = 1$. Like a "separatrix" the latter curve divides the plot into regions where the lines $A = \text{const.}$ emanate from the T -axis (for $A > 1$) and from the A -axis (for $A < 1$), respectively. The other end of the curves lies on the phase boundary between crystal and massless phases. For $A < 1$, the kink visible in the contour lines reflects the phase boundary between crystal and massive phases. In Fig. 3, the thick curves marked $= 0$ and $= 1$ correspond to phase boundaries between crystal phase and the two others. We shall return to this phase diagram in Sect. 6.

4 Calculation of observables

The standard thermodynamic observables can be computed in a straightforward manner, once the grand canonical potential (or, equivalently, the free energy) is known, see Eqs. (27) and (29)–(31). The pressure P , the (spatially averaged) baryon density ρ , the entropy density s and the energy density u are given by

$$\begin{aligned} P &= \frac{\partial \mathcal{G}}{\partial \beta} ; & \rho &= \frac{\partial \mathcal{G}}{\partial \beta} ; \\ s &= \frac{2 \beta}{\mathcal{G}} ; & u &= T s - P + \dots \end{aligned} \quad (40)$$

The x -dependence of the baryon density in the crystal phase or in the oscillating scalar condensate is somewhat harder to calculate. We start with the chiral condensate which is crucial for establishing the self-consistency of our ansatz. Using Eq. (21) and converting the sum over single particle states into an integral over the Landau energies E , we obtain

$$x = \frac{1}{e^{(\beta - \mu)/T} + 1} = \frac{S(x)}{2} \int_{E_{\text{max}}}^{\infty} \frac{Z_1}{(1 + E^2/E)^{1/2}} \frac{dE}{e^{(\beta - \mu)/T} + 1} \quad (41)$$

with μ as defined in Eq. (25) and

$$E_{\text{max}} = \frac{2}{\beta} \quad ; \quad (42)$$

Isolating the vacuum contribution ($T = 0$; $\mu = 0$) via the decomposition

$$\frac{1}{e^{(\beta - \mu)/T} + 1} = 1 - \frac{1}{e^{(\beta - \mu)/T} + 1} ; \quad (43)$$

the integration in the vacuum term can be carried out with the result

$$\begin{aligned} P &= \frac{1}{e^{(\beta - \mu)/T} + 1} = \frac{S(x)}{2} \int_{E_{\text{max}}}^{\infty} \ln \frac{2}{1 + E^2} \ln \frac{A^2}{2^2} \frac{dE}{(1 + E^2/E)^{1/2}} \\ &+ \frac{S(x)}{2} \int_{E_{\text{max}}}^{\infty} \frac{dE}{(1 + E^2/E)^{1/2}} \frac{1}{e^{(\beta - \mu)/T} + 1} + \frac{1}{e^{(\beta - \mu)/T} + 1} \end{aligned} \quad (44)$$

The self-consistency condition at finite temperature and chemical potential reads

$$S(x) = N g^2 \int_{E_{\text{max}}}^{\infty} \frac{1}{e^{(\beta - \mu)/T} + 1} \quad ; \quad (45)$$

On the other hand, the condition for $N g^2$ which follows from the vacuum gap equation in our renormalization scheme [3, 28] is

$$N g^2 = \frac{1}{\ln} \quad ; \quad (46)$$

Since the $\ln(\cdot^2)$ term on the right-hand side of Eq. (44) would already give self-consistency by itself, it might seem that this does not yield any further condition, at least in the limit $\epsilon \rightarrow 0$. However, this is not the case. Actually, the term $\ln(\cdot)$ in the chiral condensate is always "self-consistent", no matter which scalar potential $S(x)$ one puts in. This is a consequence of lowest order perturbation theory and the reason why a naive iteration of the Hartree-Fock equation does not work in the field theoretic case [19]. (Presumably, it is also related to notorious UV difficulties encountered when applying variational methods to field theories, the most famous example being Feynman's work on 3-dimensional Yang Mills theory [29].) Instead, one has to subtract the logarithmically divergent term and require that the finite terms (in the limit $\epsilon \rightarrow 0$) vanish, as has been verified for the case of the single baryon in Ref. [28] and for baryonic matter at $T = 0$ in Ref. [22]. Here, this yields the non-trivial condition

$$0 = \ln \frac{A^2}{2} \frac{Z_1^2}{2} \frac{Z_1^2}{2} \frac{1}{2} \frac{1}{2} + \frac{Z_1}{1 + \epsilon^2} \frac{Z_1}{2} \frac{dE}{(1 - E)(1 + \epsilon^2 - E)} \frac{1}{e^{(\cdot) + 1}} + \frac{1}{e^{(\cdot + \epsilon) + 1}} : \quad (47)$$

We will show analytically that this condition indeed follows from the minimization of the effective potential with respect to A and ϵ in the next section.

Let us do the analogue calculation for the baryon density, starting from Eq. (22),

$$\begin{aligned} &= \frac{X}{2} \frac{Y}{1 + \epsilon^2} \frac{1}{e^{(\cdot) + 1}} \\ &= \frac{A}{2} \frac{Z_{\text{max}}}{1 + \epsilon^2} \frac{Z_1}{2} \frac{dE}{(1 - E)(1 + \epsilon^2 - E)(E - \epsilon^2)} \frac{1}{e^{(\cdot) + 1}} + \frac{1}{e^{(\cdot + \epsilon) + 1}} \end{aligned} \quad (48)$$

Here, we have introduced the quantity r related to the ϵ -dependent part of Y , Eq. (22), as

$$r = \frac{1}{2} \frac{h}{2} \frac{dn^2(\cdot; \epsilon)}{dn^2(\cdot + K; \epsilon)} + \frac{i}{2} : \quad (49)$$

Rewrite the negative energy pieces using the decomposition (43),

$$= \text{vac} + \sim \quad (50)$$

with

$$\begin{aligned} \text{vac} &= \frac{A}{2} \frac{Z_{\text{max}}}{1 + \epsilon^2} \frac{Z_1}{2} \frac{dE}{(1 - E)(1 + \epsilon^2 - E)(E - \epsilon^2)} = \frac{1}{2} \\ \sim &= \frac{A}{2} \frac{Z_1}{1 + \epsilon^2} \frac{Z_1}{2} \frac{dE}{(1 - E)(1 + \epsilon^2 - E)(E - \epsilon^2)} \frac{1}{e^{(\cdot) + 1}} - \frac{1}{e^{(\cdot + \epsilon) + 1}} \end{aligned} \quad (51)$$

The vacuum part vac can be eliminated by subtraction. The non-trivial density \sim has to be evaluated numerically in general. Incidentally, using Eq. (22), one can easily check that its spatial average satisfies

$$h \sim i = \frac{\partial}{\partial \epsilon} \quad (52)$$

as required by thermodynamics. Since the x -dependence of the baryon density has not been discussed before, let us specialize to $T = 0$ where one can compute everything in closed form. A straightforward calculation summing over all occupied states yields (for the case of matter)

$$\sim = \frac{1}{2} \frac{K^0}{K} \left[\operatorname{dn}^2(\phi) + \operatorname{dn}^2(\phi + K) \right] - \frac{E}{K} : \quad (53)$$

This expression has the following high and low-density limits: At low density ($\phi \rightarrow 0$), we recover the result for a single baryon,

$$\sim \sim \frac{1}{4 \cosh^2(\phi)} + \frac{1}{4 \cosh^2(\phi + K)} : \quad (54)$$

At high density ($\phi \rightarrow \pi/2$), the contribution from $j_+ \bar{j}$ becomes

$$\sim \sim \frac{p_f}{2} + \frac{\ln(4p_f)}{2p_f} \cos^2(p_f x) - \frac{1}{2} : \quad (55)$$

\sim can be obtained by the substitution $\cos^2(p_f x) \rightarrow \sin^2(p_f x)$ so that to this order, the total baryon density is again constant,

$$\sim \sim \frac{p_f}{2} : \quad (56)$$

5 Analytical proof of self-consistency

In this section, we verify that the self-consistency equation (47) for the scalar potential is fulfilled provided we minimize the grand canonical potential with respect to the parameters $a = A$ and θ . To this end, we return to the gap equations (37). Using the explicit expressions for G and G_3 [Eqs. (34,35)], the gap equations can be cast into the form

$$\begin{aligned} Z &= \frac{K^p}{E} \frac{1 - \theta^2}{(1 - \theta^2)K} + \frac{1}{aG_3} \frac{\partial}{\partial a} aF \\ Z &= 2 \frac{K^p}{E} \frac{1 - \theta^2}{(1 - \theta^2)K} + \frac{2F^0}{aG_3^0} \end{aligned} \quad (57)$$

with

$$Z = \ln \frac{2(1 - \theta^2)^2}{a^2} \frac{K^p}{(1 - \theta^2)^2} : \quad (58)$$

By taking an appropriate linear combination of Eqs. (57), we cancel the first terms on the right hand side,

$$\frac{1}{2}(E - K)Z = - \frac{K}{a} \frac{\partial}{\partial a} aF - \frac{K^2(1 - \theta^2)}{a(E - (1 - \theta^2)K)} F^0 : \quad (59)$$

To proceed further, we split up F [Eq. (34)] into the contributions from the two Landau bands, $F = F_1 + F_2$. Since we need to take the derivative of these integrals with respect to θ , we find it more convenient to change integration variables such that the integration limits become θ -independent. A possible choice is

Lower band:

$$E = Z^2 + (1 - Z^2) \quad (60)$$

$$F_1(a; \beta; \gamma) = \frac{1}{2} \int_0^{Z_1} d \ln \frac{E-K}{(1-\beta)(1+\gamma^2)} \frac{1}{1+e^{\frac{p}{a}(1-\gamma^2)}} + \frac{1}{1+e^{\frac{p}{a}(1-\gamma^2)}} \quad (61)$$

Upper band:

$$E = 1 + Z^2 + \quad (62)$$

$$F_2(a; \beta; \gamma) = \frac{1}{2} \int_0^{Z_1} d \ln \frac{E-K}{(1+\beta)(1+\gamma^2)} \frac{1}{1+e^{\frac{p}{a}(1+\gamma^2)}} + \frac{1}{1+e^{\frac{p}{a}(1+\gamma^2)}} \quad (63)$$

Let us use the same integration variables in the self-consistency equation (47),

$$Z = H_1 + H_2 \quad (64)$$

with

$$H_1(a; \beta; \gamma) = \int_0^{Z_1} \frac{d}{(1-\beta)(1+\gamma^2)} \frac{p}{1-\gamma^2} \frac{1}{e^{\frac{p}{a}(1-\gamma^2)}} + \frac{1}{1+e^{\frac{p}{a}(1-\gamma^2)}} \quad !$$

$$H_2(a; \beta; \gamma) = \int_0^{Z_1} \frac{d}{(1+\beta)(1+\gamma^2)} \frac{p}{1+\gamma^2} \frac{1}{e^{\frac{p}{a}(1+\gamma^2)}} + \frac{1}{1+e^{\frac{p}{a}(1+\gamma^2)}} \quad (65)$$

Eliminating Z from Eqs. (59) and (64), the self-consistency condition can now be written in the equivalent form

$$\int_0^{Z_1} d K_1 + \int_0^{Z_1} d K_2 = 0 \quad (66)$$

If the integrands of the various integrals appearing above are abbreviated as

$$F_1 = \int_0^{Z_1} d I_1; \quad F_2 = \int_0^{Z_1} d I_2;$$

$$H_1 = \int_0^{Z_1} d J_1; \quad H_2 = \int_0^{Z_1} d J_2; \quad (67)$$

we have

$$K_i = \frac{1}{2} (E - K) J_i + \frac{K}{a} \frac{\partial}{\partial a} a I_i + \frac{K^2}{a} \frac{(1 - Z^2)}{(1 - Z^2) K} \frac{\partial}{\partial} I_i \quad (i = 1, 2) \quad (68)$$

In the remainder of the proof the more detailed structure of the integrands matters. We isolate the logarithmic factors L_i by writing

$$I_i = I_i L_i \quad (i = 1, 2) \quad (69)$$

with

$$\begin{aligned}
 L_1 &= \ln \frac{1 + e^{\frac{p}{a}(1-x^2)}}{1 + e^{\frac{p}{a}(1-x^2)}} \\
 L_2 &= \ln \frac{1 + e^{\frac{p}{a}(1+x^2)}}{1 + e^{\frac{p}{a}(1+x^2)}} \quad i \\
 I_1 &= \frac{1}{2} \frac{E = K}{\frac{1}{(1-x^2)(1+x^2)}} \\
 I_2 &= \frac{1}{2} \frac{E = K}{\frac{1}{(1+x^2)(1-x^2)}} \quad (70)
 \end{aligned}$$

Differentiation of the logarithms L_i with respect to a or i can be converted into differentiation with respect to x ,

$$\begin{aligned}
 L_1 &= \frac{2}{a} \frac{\partial L_1}{\partial} ; \quad L_1^0 = \frac{2}{1-x^2} \frac{\partial L_1}{\partial} \\
 L_2 &= \frac{2(1+x^2)}{a} \frac{\partial L_2}{\partial} ; \quad L_2^0 = 0 \quad (71)
 \end{aligned}$$

Since the J_i can also be expressed in terms of $\partial L_i = \partial$,

$$J_i = \frac{\partial L_i}{\partial} \quad (i = 1, 2) \quad (72)$$

with reduced integrands

$$J_1 = \frac{2^p - 1}{a(1-x^2)(1+x^2)} ; \quad J_2 = \frac{2^p + 1}{a(1+x^2)} ; \quad (73)$$

the general structure of K_i as far as the logarithms are concerned is therefore

$$K_i = X_i \frac{\partial L_i}{\partial} + Y_i L_i \quad (i = 1, 2) : \quad (74)$$

The X_i, Y_i are computed as follows,

$$\begin{aligned}
 X_1 &= \frac{E}{2} K J_1 + \frac{2}{a} \frac{K}{E} \frac{E}{(1-x^2)K} I_1 \\
 X_2 &= \frac{E}{2} K J_2 + \frac{2}{a} \frac{K(1+x^2)}{E} I_2 \\
 Y_i &= \frac{K}{a} I_i + \frac{K^2}{a(E(1-x^2)K)} I_i^0 \quad (i = 1, 2) \quad (75)
 \end{aligned}$$

The crucial property which one can now easily ascertain is

$$Y_i = \frac{\partial}{\partial} X_i \quad (i = 1, 2) : \quad (76)$$

This shows that the integrands K_i in Eq. (74) are total derivatives of $X_i L_i$ with respect to a . Moreover, since the functions $X_i L_i$ vanish at the respective integration boundaries,

both integrals appearing in Eq. (66) are zero. Hence self-consistency indeed follows from the gap equations. This is by no means trivial, since our variational ansatz for $S(x)$ had only two free parameters whereas the self-consistent Hartree-Fock potential corresponds to the minimum with respect to arbitrary variations of $S(x)$.

To summarize this somewhat technical section, we have found that the self-consistency condition can be expressed as a certain linear combination of the two gap equations. If one extracts the weight factors from the above calculation, the upshot is the following relationship,

$$Z + H_1 + H_2 = \frac{2K}{a^2(E - K)} \frac{\partial}{\partial a} + K \frac{\partial}{\partial K} \stackrel{!}{\sim}; \quad (77)$$

where the left hand side is the self-consistency condition and we have used

$$K \frac{\partial}{\partial K} = \frac{(1 - \frac{a^2}{E})^2}{1 - \frac{a^2}{E}} \frac{\partial}{\partial} \quad (78)$$

It thus appears that in the case at hand, self-consistency is tantamount to minimizing the free energy with respect to the single "radial" variable $\frac{a^2}{a^2 + K^2}$.

6 Phase boundaries and multicritical point

Limit ! 1, non-perturbative phase boundary

This limit is relevant for the translationally unbroken, chirally broken "massive" phase as well as for the phase boundary between crystal and massive phases. We shall expand the rescaled grand canonical potential $\tilde{\lambda}$ conveniently defined as

$$= 1 - 8^2 : \quad (79)$$

For E_{gs} and I_1 , this is straightforward,

$$^2(E_{\text{gs}} + I_1) = \frac{a^2}{4} \ln \frac{a^2}{2} \stackrel{!}{=} \frac{a^2}{4} \ln \frac{a}{\ln \frac{1}{\ln \frac{1}{\ln}} + \frac{4a^2}{\ln}} + O(2) : \quad (80)$$

For I_2 , we again invoke the same change of integration variables as in Eqs. (60) and (62). Expanding the integrand, one can perform the integration for the lowerband contribution,

$$^2 I_2 \text{low} = \frac{a}{2} \ln^h (1 + e) \ln^i \frac{1}{\ln} \frac{4a^2}{\ln} + O(2) ; \quad (81)$$

whereas for the upperband contribution this is not possible,

$$^2 I_2 \text{up} = \frac{a}{2} \int_0^{Z_1} \frac{d}{p} \ln^h \frac{1}{1 + \frac{1}{\ln}} \stackrel{!}{=} \ln^h \frac{1}{1 + e^{a^p \frac{1}{p+1}}} \ln^i \frac{1}{1 + e^{a^p \frac{1}{p+1}}} + O(2) : \quad (82)$$

Changing to the integration variable $q = a^p$ and collecting all the results then yields the following expansion,

$$\tilde{\lambda} = C_0 + C_1 \frac{1}{\ln} + O(2) ; \quad (83)$$

with

$$\begin{aligned} C_0 &= \frac{a^2}{4} \left(1 - \ln \frac{a^2}{2} \right)^! - \frac{1}{0} \int_1^{\infty} dq \ln \frac{1+e^{-\frac{p}{q^2+a^2}}}{1+e^{\frac{p}{q^2+a^2}}} \frac{p}{q^2+a^2} ; \\ C_1 &= \frac{a^2}{2} \left(1 - \ln \frac{a^2}{2} \right)^! + \frac{a}{2} \ln \frac{h}{(1+e^{-\frac{p}{q^2+a^2}})} \frac{1}{1+e^{\frac{p}{q^2+a^2}}} \\ &\quad - \frac{1}{0} \int_1^{\infty} dq \frac{a^2}{q^2+a^2} \ln \frac{1+e^{-\frac{p}{q^2+a^2}}}{1+e^{\frac{p}{q^2+a^2}}} \frac{p}{q^2+a^2} ; \end{aligned} \quad (84)$$

C_0 is recognized as the effective potential for the translationally invariant case if we identify $A = a = 1$ with the physical fermion mass. Thus $= 1$ reproduces the old solution [11] as expected. If the next-to-leading order term ($1 = \ln h$) vanishes, we are just at the phase boundary between the translationally symmetric, massive Fermi gas and the kink-antikink crystal. Hence the following two equations determine this particular phase boundary,

$$\frac{\partial}{\partial a} C_0 = 0 ; \quad C_1 = 0 ; \quad (85)$$

For the non-trivial solution with $a \neq 0$ this amounts to

$$0 = \ln \frac{a}{2} + \int_0^{\infty} dq \frac{1}{e^{\frac{p}{q^2+a^2}} + 1} + \frac{1}{e^{\frac{p}{q^2+a^2}} + 1} ; \quad (86)$$

and

$$\begin{aligned} 0 &= 1 - \ln \frac{a}{2a} - \frac{h}{2a} \ln \frac{(1+e^{-\frac{p}{q^2+a^2}})}{1+e^{\frac{p}{q^2+a^2}}} \frac{1}{1+e^{\frac{p}{q^2+a^2}}} \\ &\quad + \int_0^{\infty} dq \frac{1}{e^{\frac{p}{q^2+a^2}} + 1} + \frac{1}{e^{\frac{p}{q^2+a^2}} + 1} ; \end{aligned} \quad (87)$$

Now a can be trivially eliminated. The resulting single equation determines the relation between a and h along the phase boundary. Eq. (86) then yields a so that $(A; h)$ can all be reconstructed. The (non-perturbative) phase boundary thus obtained is shown in the phase diagram, Fig. 4. An expanded plot which reveals more details about the shape of the curve is displayed in Fig. 5.

Limit $! 0$, perturbative phase boundary

Here we are interested in the boundary between the chirally restored phase and the crystal. In Ref. [22], it has already been determined via almost degenerate perturbation theory. Let us rederive it from the full thermodynamic potential as an additional cross-check. A non-trivial calculation reveals that the integral F in Eq. (34) has the following power series expansion for $! 0$,

$$F = -\frac{1}{16} g_0 + \frac{1}{16} (g_1 - 2g_2) + O(\epsilon^6) \quad (88)$$

The g_i are functions of a and h ,

$$\begin{aligned} g_0 &= \frac{2}{6a} + \frac{2}{2a} \\ g_1 &= a \ln a + \frac{1}{2} [f(a) - f(a+)] - f(a) + f(a+) \\ g_2 &= \frac{a^2}{2} \frac{1}{a} g_1 \end{aligned} \quad (89)$$

where the function f is defined as

$$f(z) = \int_0^z dx \frac{\ln x}{1 + e^{x+z}} : \quad (90)$$

Using these results the effective potential can be approximated by

$$\sim = -\frac{1}{6} \left(\frac{2}{2} + \frac{4a^2}{32} \right) [2 \ln(2) - (a;)] \quad (91)$$

with

$$(a;) = g(a +) + g(a -) ;$$

$$g(z) = \frac{d}{dz} [f(z) - f(-z)] = \ln(2) - \text{Re} \left(\frac{1}{2} + \frac{iz}{2} \right) : \quad (92)$$

The zeroth order terms in Eq. (91) are the results for the chirally restored phase (free, massless quarks), showing the perturbative nature of the expansion in \sim (remember that $\sim = \epsilon^2$). The terms of order ϵ^4 correspond to the leading perturbative correction as evaluated in Ref. [19]. If we keep a fixed, a constrained phase boundary between crystal and massless phases can be determined by requiring that the coefficient of ϵ^4 in Eq. (91) vanishes,

$$2 \ln(2) - (a;) = 0 : \quad (93)$$

The envelope of all these curves then provides us with the true phase boundary. It can be obtained by requiring that

$$\frac{\partial (a;)}{\partial a} = 0 ; \quad (94)$$

in addition to Eq. (93). The resulting curve is included in Figs. 4 and 5.

Limit $a \rightarrow 0$, perturbative phase boundary and tricritical point

For the sake of completeness we also reproduce the phase boundary between the massive and massless homogeneous phases which is common to the new and old phase diagrams. It can be derived for example by taking the limit $a \rightarrow 0$ of Eq. (93),

$$\ln \frac{4}{2} + \text{Re} \left(\frac{1}{2} + \frac{iz}{2} \right) = 0 : \quad (95)$$

It is valid between the $\epsilon = 0$ axis and the tricritical point. The critical temperature at $\epsilon = 0$ can be inferred from Eq. (95) and coincides with the known value

$$T_c = \frac{e^c}{2} : \quad (96)$$

The tricritical point is found by letting $a \rightarrow 0$ in Eqs. (93) and (94) yielding Eq. (95) together with

$$\text{Re} \left(2; \frac{1}{2} + \frac{iz}{2} \right) = 0 : \quad (97)$$

One finds $\epsilon_t = 0.608221$; $T_t = 0.318329$; $\epsilon_c = 3.141404$ in agreement with the tricritical point of the old phase diagram. This phase boundary has also been plotted in Figs. 4 and 5.

Let us assume $a \neq 0$ for arbitrary λ , vicinity of tricritical point

Here, we expand the thermodynamic potential in a without assuming anything about λ . This should be useful in the vicinity of the multicritical point. After a lengthy computation one finds

$$\sim = \frac{1}{6} \frac{a^2}{2} \frac{\ln \frac{1}{4}}{B_1} \text{Re} \frac{1}{2} + \frac{i}{2} \frac{\#}{24^3 B_2 \text{Re}} \frac{1}{2} + \frac{i}{2} + \frac{a^6}{1920} B_3 \text{Re} \frac{1}{2} + \frac{i}{2} \quad : \quad (98)$$

The λ -dependence is encoded in the coefficients B_i given by

$$\begin{aligned} B_1 &= 1 \frac{1}{2}^2 \frac{E}{K} \\ B_2 &= 1 \frac{3}{8}^4 \frac{E}{K} 1 \frac{1}{2}^2 \\ B_3 &= 1 \frac{9}{8}^4 \frac{5}{16}^6 \frac{E}{K} 1 \frac{3}{8}^4 \quad : \end{aligned} \quad (99)$$

The Polygamma functions in Eq. (98) appear as a consequence of Eq. (92). Maximizing \sim with respect to a and λ along the lines sketched at the end of Sect. 3 yields the following explicit results: Provided $a \neq 0$, we find

$$a^2 = 40^2 G_1(\lambda) \frac{\text{Re} \frac{1}{2} + \frac{i}{2}}{\text{Re} \frac{1}{2} + \frac{i}{2}} \quad (100)$$

with

$$G_1(\lambda) = \frac{1 \frac{1}{2}^2 \frac{E}{K} 1 \frac{1}{2}^2}{1 \frac{3}{2}^2 + \frac{1}{2}^4 \frac{E}{K} 1 \frac{3}{8}^4} \quad (101)$$

and the limits

$$G_1(0) = \frac{3}{5}; \quad G_1(1) = \frac{4}{3} \quad (102)$$

If the right-hand side of Eq. (100) is positive, there is a non-trivial solution for a . The equation which determines λ [see Eq. (39)] in turn reads

$$\ln \frac{1}{4} = \text{Re} \frac{1}{2} + \frac{i}{2} \frac{5}{6} G_2(\lambda) \frac{\text{Re} \frac{1}{2} + \frac{i}{2}}{\text{Re} \frac{1}{2} + \frac{i}{2}} \quad (103)$$

with

$$G_2(\lambda) = \frac{1 \frac{1}{2}^2 + \frac{5}{8}^4 + \frac{3}{8}^6 \frac{E}{K} 1 \frac{3}{2}^2 + \frac{7}{8}^4 \frac{3}{16}^6 1^2 \frac{E}{K} 1 \frac{1}{2}^2}{1 \frac{3}{2}^2 + \frac{1}{2}^4 \frac{E}{K} 1^2 + \frac{3}{8}^4} \quad (104)$$

and the limits

$$G_2(0) = \frac{9}{5}; \quad G_2(1) = \frac{2}{3} \quad (105)$$

The two "new" phase boundaries correspond to $\alpha = 0; 1$. By using Eqs. (103) and (105), one can plot $T = 1/\alpha$ against α starting for $\alpha_t = 1.910668$ and construct these phase boundaries near the Lifshitz point. The 3rd, "old" phase boundary follows similarly from Eq. (95) for α_t . Finally, in the vicinity of the Lifshitz point, we can expand $(T; \alpha)$ around $(T_t; \alpha_t)$ and derive the (approximate) phase boundaries in closed analytical form. Starting from Eq. (103), we find to second order

$$\ln \frac{1}{\alpha} = A_1 (\alpha - \alpha_t) + A_2 (\alpha - \alpha_t)^2 \quad (106)$$

with

$$\begin{aligned} A_1 &= \frac{1}{2} \frac{\text{Im}}{\text{Re}} \left(1; \frac{1}{2} + \frac{i}{2} \right) \\ A_2 &= G_2 \left(\frac{5}{24} \right) \frac{\text{Im}}{\text{Re}} \left(3; \frac{1}{2} + \frac{i}{2} \right) \frac{i_2}{4; \frac{1}{2} + \frac{i}{2}} \end{aligned} \quad (107)$$

The equation for lines of constant α then reads

$$T - T_t = \frac{A_1 T_t}{t A_1 + T_t} (\alpha - \alpha_t) - \frac{(A_1^2 - 2A_2) T_t^2}{2(t A_1 + T_t)^3} (\alpha - \alpha_t)^2 : \quad (108)$$

The linear term is independent of α , so that all curves enter the Lifshitz point with the same slope. The quadratic term describes the α -dependence of the curvature and changes sign as a function of α . The limiting cases $\alpha = 0; 1$ yield the approximate phase boundaries in closed form. Furthermore, Eq. (100) shows that α^2 is linear in $\alpha - \alpha_t$. This translates into the behaviour

$$A(\alpha - \alpha_t)^{1/2} \quad (109)$$

along the phase boundaries and the corresponding critical exponent $1/2$ as expected for mean field theory.

Finally, we derive a Ginzburg-Landau type effective action near the Lifshitz point from the Taylor expansion of the grand canonical potential in powers of α . For this purpose, we compute spatial averages of powers of S and its derivatives (keeping all even terms up to order A^6). Upon comparing the (analytical) results of such a calculation with Eqs. (99), we find the simple relations

$$\begin{aligned} B_1 &= \frac{1}{2A^2} h S^2 i \\ B_2 &= \frac{3}{8A^4} h S^4 i + h (S^0)^2 i \\ B_3 &= \frac{5}{16A^6} h S^6 i + \frac{1}{2} h (S^0)^2 i + 5h S^2 (S^0)^2 i \end{aligned} \quad (110)$$

This enables us to write down a Ginzburg-Landau effective action as follows,

$$\begin{aligned} e &= -\frac{1}{6} T^2 - \frac{1}{2} S^2 \ln(4/T) + \text{Re} \left(\frac{1}{2} + \frac{i}{2} \frac{1}{T} \right) \\ &\quad - \frac{1}{2^6 3 T^2} S^4 + (S^0)^2 \text{Re} \left(2; \frac{1}{2} + \frac{i}{2} \frac{1}{T} \right) \\ &\quad + \frac{1}{2^{11} 3^5 T^4} S^6 + \frac{1}{2} (S^0)^2 + 5S^2 (S^0)^2 \text{Re} \left(4; \frac{1}{2} + \frac{i}{2} \frac{1}{T} \right) \end{aligned} \quad (111)$$

(This result can be applied to the translationally symmetric solution by simply dropping all the derivatives of S .) At the tricritical point, both the S^2 and $S^4 + (S^0)^2$ terms vanish, see Eqs. (95) and (97). This is the reason why we had to include terms up to the order S^6 .

7 Relation to condensed matter physics

In a previous paper, we have pointed out that GN type models can also be reinterpreted as relativistic superconductors [30]. This is due to a 2-dimensional remnant of the Pauli-Gursey symmetry of massless fermions [31, 32]. It allows us to define "particle" and "antiparticle" independently for left-handed and right-handed quarks. Models with fermion-antifermion pairing (chiral condensate) and fermion-fermion pairing (Cooper pairs) can then be mapped onto each other by a "duality" transformation. The phase diagram which we have been discussing above is equivalent to the phase diagram of a theory with Lagrangian

$$L = \frac{(i) \phi}{2} + \frac{g^2}{2} \left(\frac{(i)y}{R} \frac{(i)y}{L} + \frac{(i)}{L} \frac{(i)}{R} \right)^2; \quad (112)$$

provided we replace the chemical potential $\mu_R + \mu_L$ by the axial chemical potential $\mu_5 = \mu_R - \mu_L$ (see Ref. [30]). The kink-antikink phase of the GN model can then be identified with the Larkin-Ovchinnikov-Fulde-Ferrel (LOFF) phase [33, 34] of the dual model. Such inhomogeneous superconductors have recently attracted considerable attention in the context of QCD (for a current review article, see Ref. [35]).

Actually, there is yet another kind of connection between the GN model and non-relativistic condensed matter systems which is even more surprising. Although the GN model is mentioned occasionally in the corresponding condensed matter literature, it seems that this close relationship has never been exploited in any systematic way. The physics of the problems we have in mind is totally different from the GN model, yet the mathematical analogies are striking. Let us discuss a few pertinent references which we came across when looking for parallels between the phase diagram of the GN model and that of quasi-one-dimensional solid state systems. Incidentally, this may be regarded as a continuation of the work of Jackiw and Schriener [36] on kinks in condensed matter and relativistic field theories to finite kink densities.

The first example is a 1981 paper by Mertsching and Fischbeck on the Peierls-Frohlich model [37]. These authors address the quasi-one-dimensional Frohlich model with a nearly half-filled band, an electron-phonon system. They are interested in the phase diagram, notably the transition between commensurate-incommensurate charge density waves, using a mean field approximation. There seems to be a mathematical one-to-one correspondence between this system and the GN model. The authors of Ref. [37] have also found the analytic solution to the mean field equation, guided by the Landau expansion around the triple point (which is called Leung point [38] in this context). Crucial for the close correspondence with a relativistic field theory are evidently a continuum approximation (the lattice constant acts as inverse cut-off and is taken to 0) and a linearization of the electron dispersion relation near the Fermi surface (simulating "ultrarelativistic kinematics"). In

appropriate units, the results are identical to ours, as far as we can tell.

In a subsequent paper, Machida and Akanishi [39] used the phase diagram of Ref. [37] in a different physics context: They studied the interplay of superconductivity and ferromagnetism in ErRh_4B_4 (Erbium-Rhodium-Boride). Thanks to a number of approximations (in particular the one-dimensional band model with linear dispersion) they managed to reduce this problem mathematically to the Peierls-Frohlich model. For real order parameter, their results are again fully equivalent to ours for the GN model, except that now one has to use another dictionary: The Dirac equation corresponds to the Bogoliubov-deGennes equation, particle/antiparticle degrees of freedom to spin (which exists in a quasi-one-dimensional world), chemical potential to magnetic field, baryon density to spin polarization. Our three phases (massive, crystal and massless) correspond to their BCS, "sn" and normal phases, respectively. The order parameter at $T = 0$ looks different from ours at first sight. However, the two expressions can be converted into each other by Landen's transformation for Jacobi functions [25] in the form

$$\frac{\text{sn}(\cdot; \cdot)\text{cn}(\cdot; \cdot)}{\text{dn}(\cdot; \cdot)} = \frac{1}{\sqrt{1 - \frac{1}{\text{sn}^2(1 + \frac{1}{\text{sn}^2})}}} \frac{\text{sn}^0(\cdot; \cdot)}{\sqrt{1 + \frac{1}{\text{sn}^2(1 + \frac{1}{\text{sn}^2})}}} : \quad (113)$$

Not only the phase boundaries, but all observables can be identified if one keeps in mind the above mentioned dictionary. Nevertheless, there are subtle differences which show that one should not take over results blindly: The authors of Ref. [39] also discuss complex order parameters, in particular a helical phase. In the discrete chiral GN model, the order parameter is always real. In the continuous chiral NJL_2 model, it can be complex and we have indeed found a helical phase [15], but the results for the phase diagram are different. Here apparently the quantitative correspondence between relativistic field theory and solid state physics ends due to certain differences in dynamics.

As a third example, we should like to mention the more recent work of Buzdin and Kadkhahi [40]. They derive the Ginzburg-Landau theory for nonuniform LOFF superconductors near the tricritical point in the $(T; H)$ -phase diagram in one, two and three dimensions. If we take their result for one dimension and specialize it to a real order parameter, we find perfect agreement between our Eq. (111) and their Eq. (3) in appropriate units (a discrepancy in the sign of the $j \dot{f}$ term must be due to a misprint). We have to identify their magnetic field H_0 with our chemical potential. One can find many more similar studies in the literature, see e.g. the recent review article on stripe phases [41].

Finally, when browsing through the literature on superconductivity, we were am used to discover that the "old" phase diagram of the GN model (assuming unbroken translational invariance) is ubiquitous in textbooks and articles on BCS theory (see e.g. Ref. [42], Fig. 6.2). It seems to go back to a 1963 paper [43] which predates the original GN paper by more than one decade and the first published GN phase diagram by more than two decades.

Summarizing, we find it gratifying that the GN model with its simple Lagrangian gives rise to such a complex and physically rich phase diagram. Its structure seems to be mirrored by a variety of quasi-one-dimensional condensed matter systems. With hindsight, one

might ask the question why it took much longer to solve the same mathematical problem in relativistic quantum field theory than in condensed matter physics. We feel that this is due to the almost exclusive use of path integral methods in particle physics. Apparently, these methods are not yet developed enough to yield non-trivial saddle points with unexpected symmetry breakdown as in the present case. By contrast, canonical mean-field calculations offer a rich spectrum of approximate methods (variational, numerical etc.) which can be successively refined and used to nail down eventually the exact solution as in the case at hand. It is probably not accidental that we arrived at the phase diagram of the GN model using Hartree-Fock methods akin to the standard tools of condensed matter physics.

References

- [1] D. J. Gross and A. Neveu, Phys. Rev. D 10, 3235 (1974).
- [2] G. 't Hooft, Nucl. Phys. B 72, 461 (1974).
- [3] V. Schon and M. Thies, in: *At the frontier of particle physics: Handbook of QCD, Boris Ioffe Festschrift*, ed. by M. Shifman, Vol. 3, ch. 33, p. 1945, World Scientific, Singapore (2001).
- [4] Y. Nambu and G. Jona-Lasinio, Phys. Rev. 122, 345 (1960); *ibid.* 124, 246 (1961).
- [5] C.G. Callan, S. Coleman, D.J. Gross, and A. Zee, unpublished (referred to by [6]).
- [6] R.F. Dashen, B. Hasslacher, and A. Neveu, Phys. Rev. D 12, 2443 (1975).
- [7] L.L. Salcedo, S. Levit and J.W. Negele, Nucl. Phys. B 361, 585 (1991).
- [8] F. Lenz, M. Thies, S. Levit, and K. Yazaki, Ann. Phys. (N.Y.) 208, 1 (1991).
- [9] B.J. Harrington and A.Y.ildiz, Phys. Rev. D 11, 779 (1975).
- [10] R.F. Dashen, S.K. Ma, and R.Rajaraman, Phys. Rev. D 11, 1499 (1975).
- [11] U. Wöl, Phys. Lett. B 157, 303 (1985).
- [12] T.F. Tremblay, Phys. Rev. D 39, 679 (1989).
- [13] A. Barducci, R. Casalbuoni, M. Modugno, G. Pettini, and R. Gatto, Phys. Rev. D 51, 3042 (1995).
- [14] A. Chodos, R.L. Jaffe, K. Johnson, C.B. Thorn, and V.F. Weisskopf, Phys. Rev. D 9, 3471 (1974).
- [15] V. Schon and M. Thies, Phys. Rev. D 62, 096002 (2000).
- [16] I. Kabanov, Nucl. Phys. B 262, 133 (1985).

[17] K. Ohwa, *Phys. Rev. D* 65, 085040 (2002).

[18] A. Brzoska and M. Thies, *Phys. Rev. D* 65, 125001 (2002).

[19] M. Thies and K. Urlichs, *Phys. Rev. D* 67, 125015 (2003).

[20] R M. Homreich, M. Luban and S. Shtrikman, *Phys. Rev. Lett.* 35, 1678 (1975).

[21] A W. Overhauser, *Adv. in Phys.* 27 (1978) 343.

[22] M. Thies, [hep-th/0308164v2](#), to appear in *Phys. Rev. D*.

[23] E. T. Whittaker and G. N. Watson, *A Course of Modern Analysis*, Cambridge University Press (1980).

[24] G. V. Dunne and J. Feinberg, *Phys. Rev. D* 57, 1271 (1998)

[25] M. Abramowitz and I. Stegun (Eds.), *Handbook of Mathematical Functions*, Dover, New York (1990).

[26] H. Li, D. Kusnezov and F. Iachello, *J. Phys. A: Math. Gen.* 33, 6413 (2000).

[27] <http://functions.wolfram.com/09.01.18.0012.01>

[28] R. Pausch, M. Thies and V. Dolman, *Z. Phys. A* 338, 441 (1991).

[29] R P. Feynman, *Nucl. Phys. B* 188, 479 (1981).

[30] M. Thies, *Phys. Rev. D* 68, 047703 (2003).

[31] W. Pauli, *Nuovo Cim.* 6, 205 (1957).

[32] F. Gursey, *Nuovo Cim.* 7, 411 (1958).

[33] A. I. Larkin and Yu N. Ovchinnikov, *Sov. Phys. JETP* 20, 762 (1965).

[34] P. Fulde and R A. Ferrell, *Phys. Rev.* 135, 550 (1964).

[35] R. Casalbuoni and G. Nardulli, [hep-ph/0305069](#).

[36] R. Jackiw and J.R. Schrieffer, *Nucl. Phys. B* 190 [FS3], 253 (1981).

[37] J. M. Ertshing and H. J. Fischbeck, *phys. stat. sol. (b)* 103, 783 (1981).

[38] M. C. Leung, *Phys. Rev. B* 11, 4272 (1975).

[39] K. Machida and H. Nakanishi, *Phys. Rev. B* 30, 122 (1984).

[40] A. I. Buzdin and H. Kachkachi, *Phys. Lett. A* 225, 341 (1997).

[41] S. I. Mukhin and S. I. Matveenko, *Int. J. Mod. Phys. B* 17, 3749 (2003).

[42] D. Saint-James, G. Sarma and E. J. Thomas, *Type II Superconductivity*, Pergamon Press (1969), p. 160.

[43] G. Sarma, *J. Phys. Chem. Solids* 24, 1029 (1963).

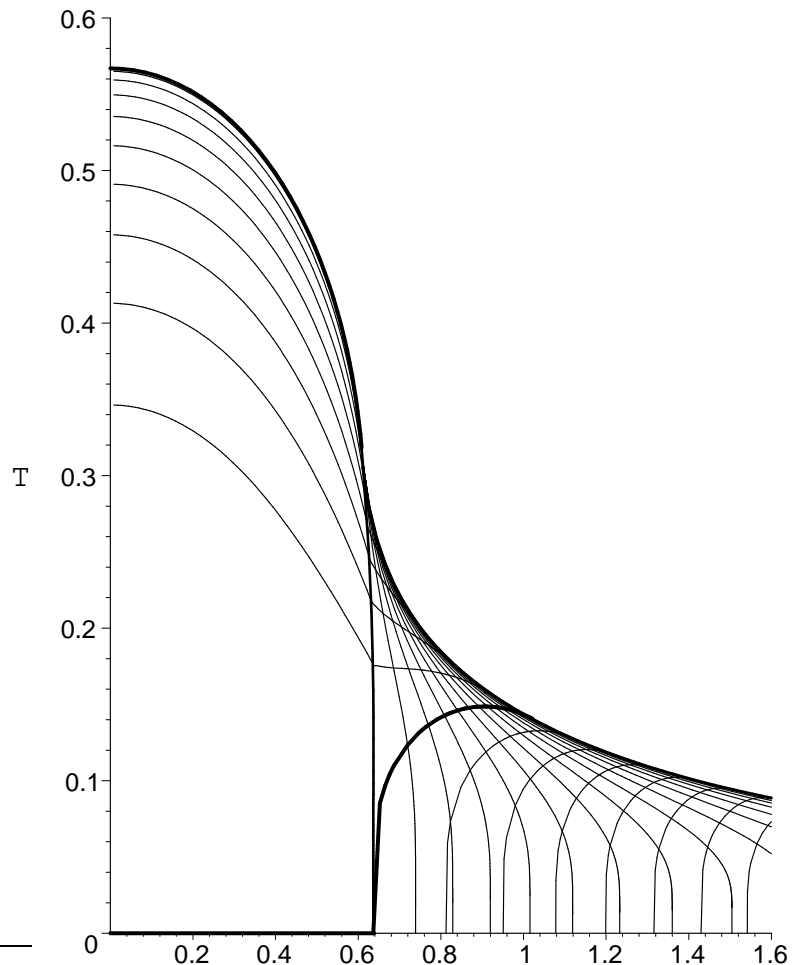


Figure 1: Lines of constant A and β in the $(\beta; T)$ -plane, obtained by minimizing the grand potential. See Figs. 2 and 3 for more details.

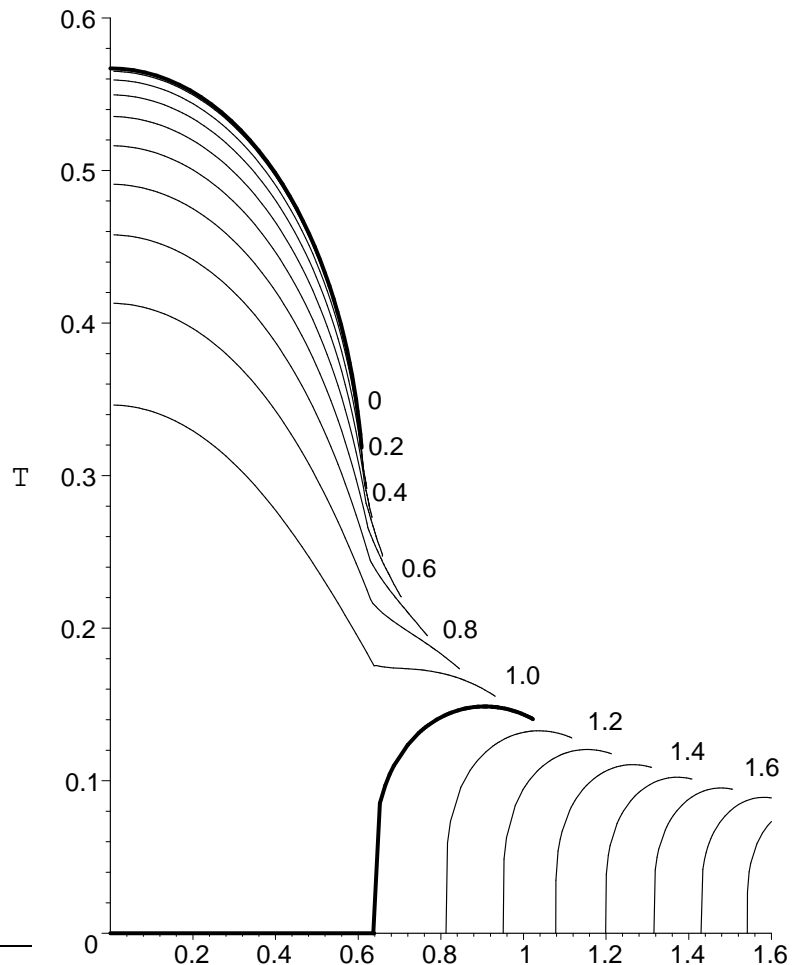


Figure 2: Contour lines $A = \text{const.}$ in the $(\cdot; T)$ -plane. Thick lines: $A = 0$ and $A = 1$. A ranges from 0 to 1.7, the line spacing is $A = 0.1$.

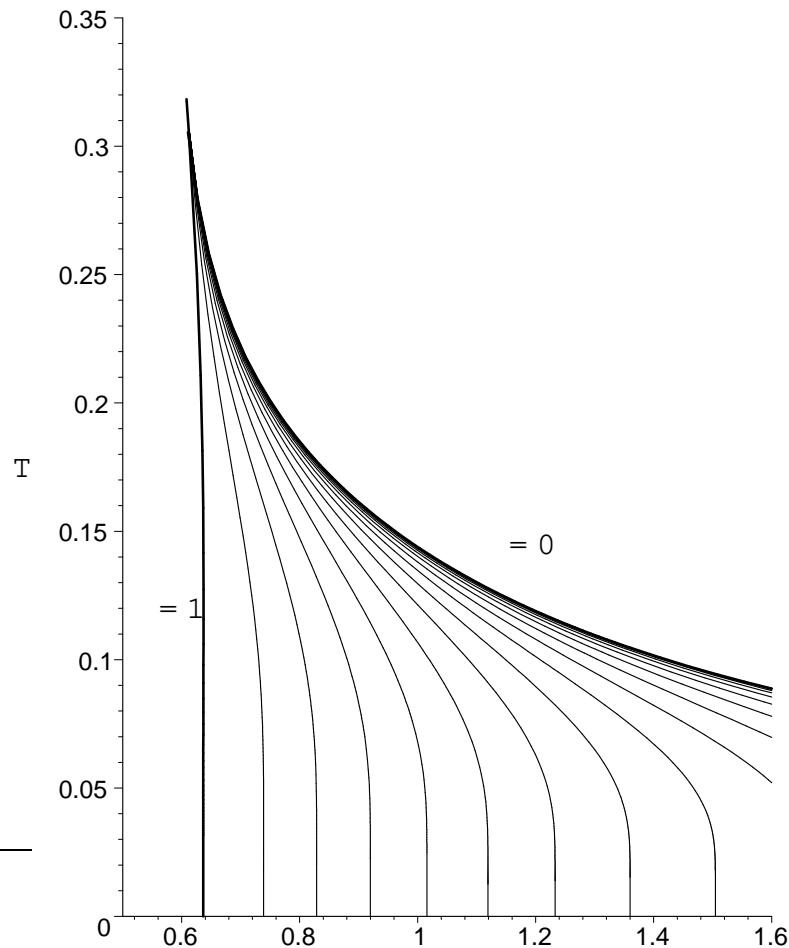


Figure 3: Contour lines $\beta = \text{const.}$ in the crystal phase. The phase boundaries are $\beta = 0$ and $\beta = 1$, adjacent lines differ by $\beta = 0.05$. All lines end at the tricritical point.

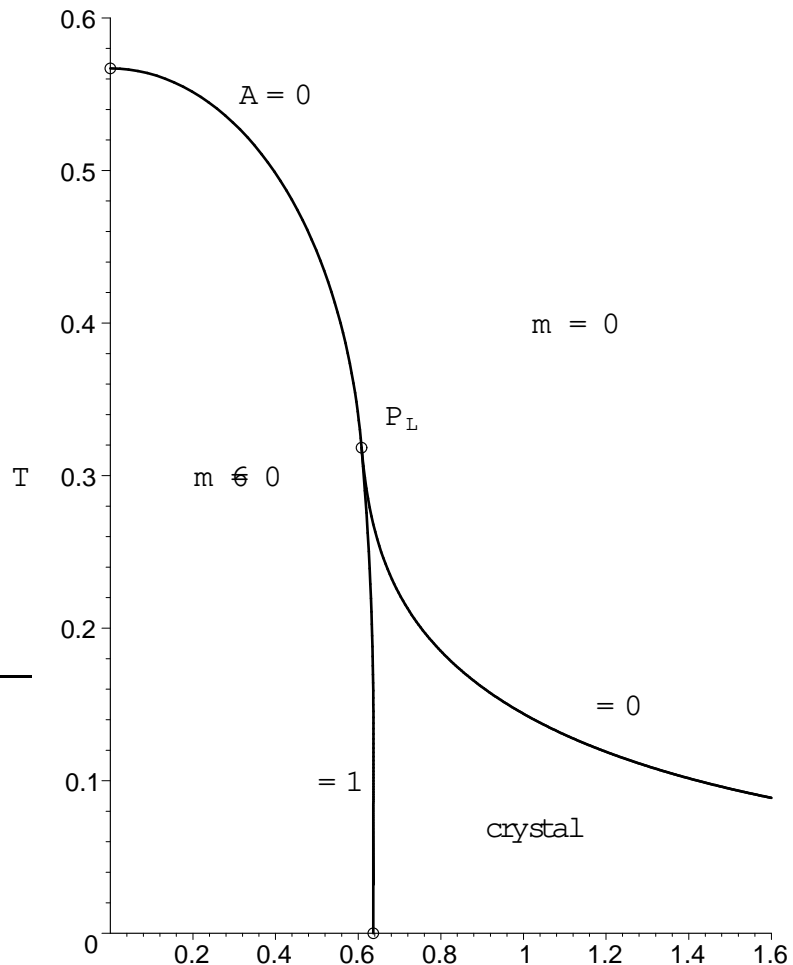


Figure 4: Phase diagram of the GN model, computed with the help of Eqs. (86), (87), (93), (94), (95). All phase boundaries are second order transitions, P_L is the Lifshitz point.

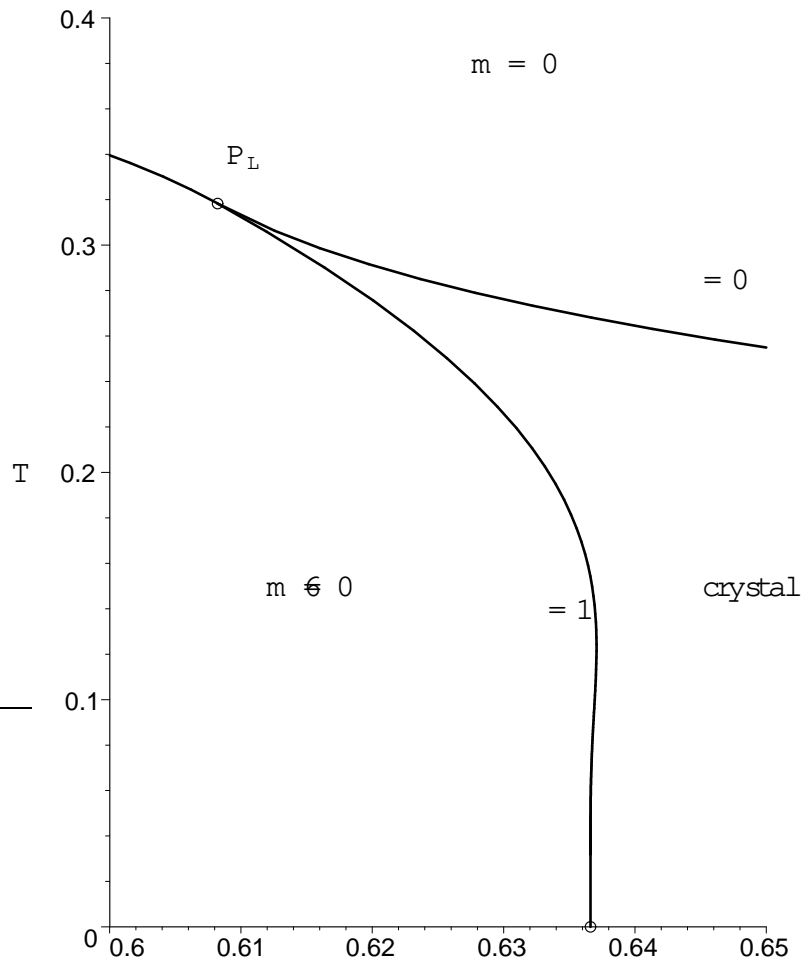


Figure 5: More detailed view of the phase boundary between homogeneous and periodic ordered phases ($= 1$). Notice the different scale on the ϵ -axis as compared to Fig. 4.